8-1976

Magnetization of NixCu$_2$-xMnSn

Richard A. MacDonald

MAGNETIZATION OF $Ni_xCu_{2-x}MnSn$

MAGNETIZATION OF $Ni_x Cu_{2-x} MnSn$

By

RICHARD A. MacDONALD, B.Sc.

· A Thesis

Submitted to the School of Graduate Studies

in Partial Fulfilment of the Requirements

for the Degree

Master of Science

McMaster University

August 1976

1977

MASTER OF SCIENCE (1976) McMASTER UNIVERSITY
(Physics) Hamilton, Ontario

TITLE: Magnetization of $Ni_xCu_{2-x}MnSn$

AUTHOR: Richard A. MacDonald, B.Sc. (St. Francis Xavier
University)

SUPERVISOR: Dr. C. V. Stager

NUMBER OF PAGES: vii, 35

ABSTRACT

The magnetization of the Heusler alloys $Ni_xCu_{2-x}MnSn$ has been measured. These alloys, of the form X_2YZ, have been investigated in order to determine the X site dependence of the interactions which are responsible for the ferromagnetism. It is seen that the Curie temperatures vary nonlinearly with composition suggesting that the short range interactions which determine them vary in a similar manner. Saturation moments are found to remain constant; however, a decrease in paramagnetic moment as the copper concentration is increased, is attributed to disorder.

ACKNOWLEDGEMENTS

I wish to thank my supervisor Dr. C. V. Stager for his assistance and encouragement especially during those times when experimental problems seemed overwhelming. I also wish to thank Mr. Jim Garrett who helped with the sample preparation and Mr. John Neimanis who managed to keep the magnetometer cooperative. This work I dedicate to my wife Nan who listened so patiently to many monologues on Heusler alloys and provided the inspiration necessary to keep the research in its proper perspective.

TABLE OF CONTENTS

LIST OF ILLUSTRATIONS

INTRODUCTION

Heusler alloys have been of interest to researchers in magnetism since their discovery by O. Heusler in 1898. These ternery alloys are of the form X_2YZ where Y is Mn. X is usually Cu, Co, Ni, Pd, Pt, or Rh and Z is In, Sn, Sb, Al, Ge, or Ga. Most of these alloys form a $L2_1$ crystal structure with an F.C.C. lattice of lattice parameter close to six angstroms. Figure 1 illustrates the crystal structure. The alloys which contain manganese are mostly ferromagnetic with saturation moments of four Bohr magnetons per formula unit (Oxley et al. 1963). In agreement with the literature this will be referred to as 4 u_B/molecule.

Neutron diffraction experiments (Webster 1967) support the assumption that the magnetic moment is localized entirely on the manganese site except for the alloys containing cobalt (Ziebeck and Webster 1974). Extensive work has been done measuring hyperfine fields in these alloys in order to obtain information on the interactions which are responsible for the ferromagnetism. There is a recent review article (Campbell 1975). Since the manganese atoms are too far apart to be coupled by direct interactions of the d electrons it is thought that some form of indirect interaction through the conduction band such as the R-K-K-Y interaction is important for ferromagnetism. Caroli and Blandin (1966) have proposed a double resonance model, however it has not been found especially accurate in comparison with experiments on hyperfine fields (Campbell, 1975).

Figure 1

The $L2_1$-Heusler crystal structure. For

$Ni_xCu_{2-x}MnSn$: X is Ni or Cu, Y is Mn and

Z is Sn.
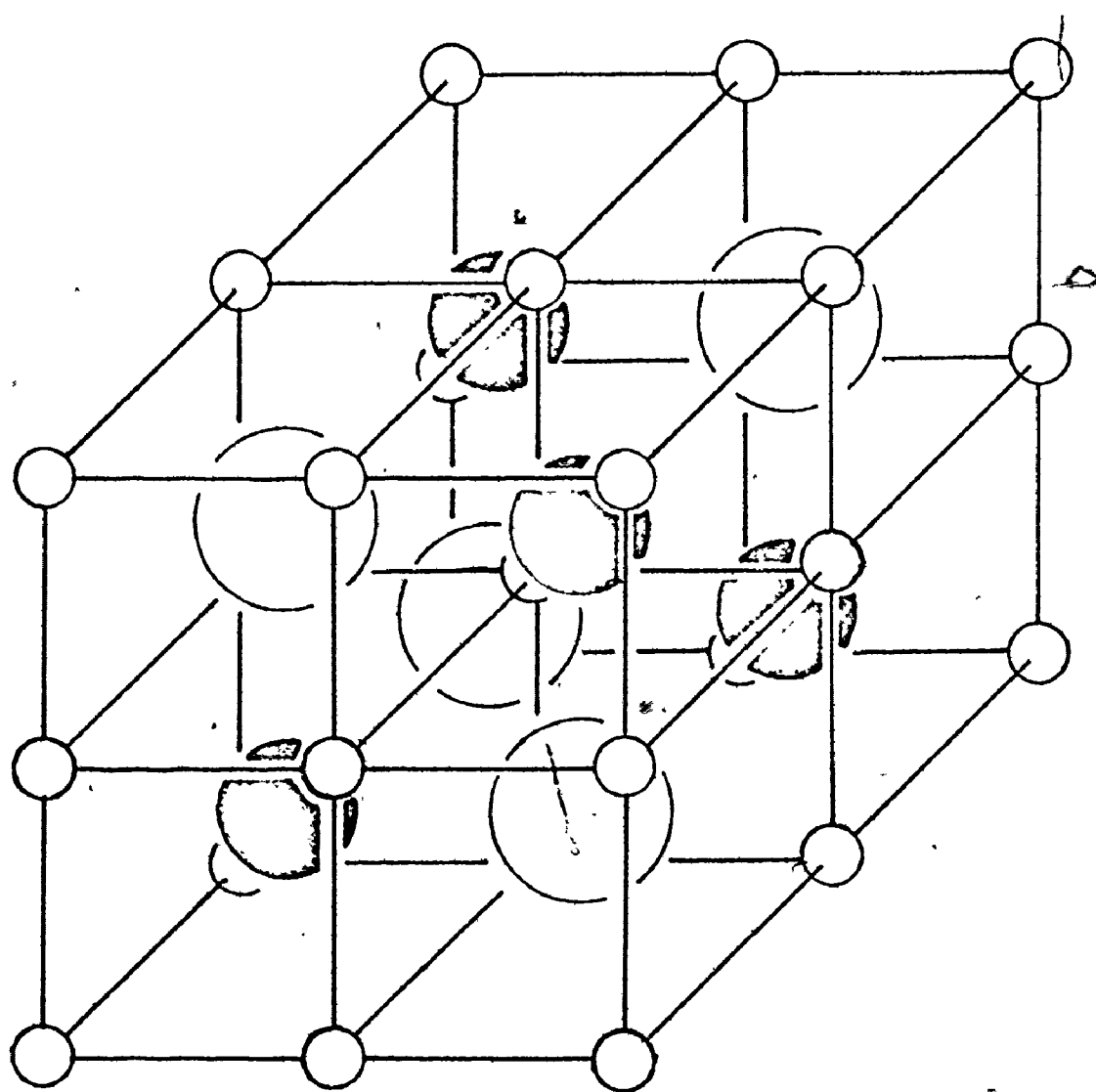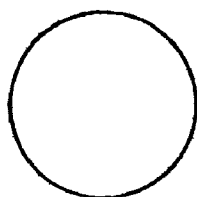
X   Z   Y
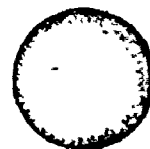
Bulk magnetization measurements are useful in providing information about the magnetic properties of these alloys. Usually the magnetic properties are measured as the composition of the alloy under study is changed. One method of doing this is to vary the composition between two closely related alloys while retaining the Heusler structure. This is possible if the atoms on only one lattice site are changed.

Most experiments of this type are done by changing the Y site component. Campbell and Stager (1976) have determined the composition dependence in the system $Ni_2Mn_xTi_{1-x}Sn$. This series of alloys varies from ferromagnetic Ni_2MnSn to paramagnetic Ni_2TiSn while maintaining the local moment characteristic of 4 u_b/Mn atom. Booth and Pritchard (1975) have investigated $Co_2Ti_xGa_{1-x}Ga$ and attribute the onset of ferromagnetism at x = 0.5 to changes in electron concentration rather than crystal structure. Endo et al. (1972) have estimated the s-d interactions in the dilute system $Cu_2Ni_{1-x}Mn_xSn$.

In the Heusler alloys containing manganese it would seem at first glance that the X site is relatively unimportant in determining the magnetic properties. In Ni_2MnSn for instance, Ni only contributes at most one electron to the conduction band. Noda and Ishikawa (1976) have fitted the magnon dispersion curves for Ni_2MnSn and Pd_2MnSn. From these fits they have determined the exchange interactions up to eighth nearest neighbours. They find that the first and second near neighbour interactions are inconsistent with the s-d model and suggest that the X site atom plays a crucial role in determining these short range

interactions. It is these interactions which largely affect the Curie temperature.

The purpose of this thesis is to investigate the effect of systematically varying the X site component in a representative Heusler system. The system $Ni_xCu_{2-x}MnSn$ was chosen for several reasons. There is a large difference in Curie temperatures between Ni_2MnSn and Cu_2MnSn. Both of these alloys are local moment ferromagnets with the moment concentrated entirely on the manganese site. Experience in the laboratory indicated that Ni_2MnSn was easy to make with reproducible results. The alloy components are relatively inexpensive and readily obtainable. There is one disadvantage, however. Oxley et al (1963) have reported that high temperature magnetization measurements of Cu_2MnSn can not be performed because of irreversible precipitation of another phase as the temperature is increased. The precipitation was observed by metallographic examination as well as by X-ray powder methods. Since Ni_2MnSn does not show this effect it was hoped that the majority of the intermediate Ni-CuMnSn alloys would be free from this type of effect. Attempts were made to make the alloys of In instead of Sn but these were unsuccessful.

The remainder of this thesis is divided into five parts, Chapters 2 to 6 inclusive. Chapter 2 is a section on theory which contains an account of effective field theory. The third chapter is a description of sample preparation and experimental apparatus. The fourth chapter contains the data which is discussed in Chapter 5. Finally conclusions and suggestions for further research are included in Chapter 6.

CHAPTER 2

THEORY

In this section some relevant theory is presented. In particular effective field theory is discussed with application to the magnetization measurements at temperatures above the Curie point. A method for analyzing low temperature magnetization measurements is also discussed.

EFFECTIVE FIELD THEORY

This description of effective field theory is similar to that found in Effective Field Theories of Magnetism (Smart 1966).

Above its Curie temperature a local moment ferromagnet can be adequately described in the effective field approximation. In its most simple form this theory considers only one magnetic atom and replaces its interaction with the rest of the crystal by an effective field. This is also sometimes called a molecular field. The exchange interaction energy between two spins $\underline{S}_i$ and $\underline{S}_j$ can be written as

$$E = -2 J_{ij} \underline{S}_i \cdot \underline{S}_j \tag{1}$$

where J_{ij} is the exchange integral for the i and j'th spins. If the exchange integrals are assumed isotropic then the single particle Hamiltonian for a given spin i may be written

5

$$H_i = -2 \sum_r J_r \, \underline{S}_i \cdot \sum_j^{Z_r} \underline{S}_j \qquad (2)$$

where it is assumed that all first neighbour interactions are the same, etc. Z_r is the number of r'th nearest neighbours. Since the high temperature results may be influenced by more than just near neighbour interactions we allow the possibility of further interactions by the summation over r.

To replace these interactions by an effective field $\underline{H}_e$ we require that H_i has the form

$$H_i = -g \, u_B \, \underline{S}_i \cdot \underline{H}_e . \qquad (3)$$

Equating equations (2) and (3) we can identify

$$\underline{H}_e = \frac{2}{g u_B} \sum_r J_r \sum_j^{Z_r} \cdot \underline{S}_j . \qquad (4)$$

For the effective field approximation each spin $\underline{S}_j$ may be replaced by its average value $<\underline{S}>$. Since the total magnetic moment of the crystal is

$$\underline{M} = N \, u_B \, g <\underline{S}> \qquad (5)$$

where N is the number of spins $<\underline{S}>$, then

$$\underline{H}e = \frac{2}{g^2 \, u_B^2 \, N} \sum_r J_r \, Z_r \, \underline{M} \qquad (6)$$

Consider also an applied field $\underline{H}_o$ so that the total field acting on the i'th spin is

$$\underline{H} = \underline{H}_o + \underline{H}_e \tag{7}$$

For simplicity assume $\underline{S}$, $\underline{H}$, $\underline{H}_o$, $\underline{H}_e$ and $\underline{M}$ lie along the z axis. The one atom Hamiltonian now becomes

$$H_i = -g\ u_B\ S_z\ H \tag{8}$$

with eigenvalues $E = -g\ u_B m\ H$, $m = S, S-1, ---- -S$. The partition function of the system is

$$Q_s = \sum_m e^{g u_B m H / kT} = \frac{\sinh((2S + 1)x/2S)}{\sinh(x/2S)} \tag{9}$$

where $x = \dfrac{g\ u_B\ S\ H}{kT}$

The total magnetic moment is defined to be

$$M = kT\ (\partial \ln Q_n / \partial H)_T \tag{10}$$

where $Q_n = (Q_s)^N$. Substituting equation (9) into equation (10) we find that

$$M = g\ u_B\ N\ S\ ((2S + 1)/2S \coth (2S + 1)x/2S - 1/2S \coth (x/2S)) \tag{11}$$

In the high temperature region of interest $x \ll 1$. For small arguments y, $\coth y \cong 1/y + y/3 + ------$
so that $(2S + 1)/2S \coth ((2S + 1)x/2S) - 1/2S \coth (x/2S) = x(S + 1)/3S$
Now $M(x \ll 1) \cong g\ u_B\ N\ S\ (x/3S\ (S + 1))$ so that

$$M(x<<1) = \frac{N\ g^2\ u_B^2\ H}{3kT}\ S(S+1) \tag{12}$$

This expression may be written as $M = \frac{C\ H}{T}$ (13)

where the Curie constant C is equal to $C = \frac{N\ g^2\ u_B^2\ S(S+1)}{3k}$

Substituting (7) and (6) into (13) gives

$$\frac{M}{H_o} = \frac{C}{T-2\sum_r Z_r\ J_r\ C/(Ng^2\ u_B^2)} = \frac{C}{T-\theta} \tag{14}$$

where the paramagnetic Curie temperature θ is given by

$$\theta = \frac{2C\sum_r Z_r\ J_r}{N\ g^2 u_B^2} = 2\sum_r \frac{Z_r\ J_r\ S(S+1)}{3k} \tag{15}$$

From equation (14) it is seen that the inverse magnetization 1/M varies linearly with T once the condition that x<<1 is met. At sufficiently high temperatures a plot of 1/M versus T at constant applied field H_o gives a straight line of slope 1/C with intercept at $T = \theta$. From equation (15) it can be seen that θ gives a measure of the interactions responsible for the ferromagnetism. The slope of the graph equal to 1/C determines the effective paramagnetic moment. This is defined as

$$P = g(S(S+1))^{1/2} = (3kC/Nu_B^2)^{1/2}$$

A measure of the paramagnetic moment gives an indication of the average spin S of the system.

MEASUREMENT OF SATURATION MAGNETIZATION

Because of the presence of domains in ferromagnetic materials, the saturation magnetization cannot be measured directly. Application of a large external magnetic field is necessary to remove the domain walls and allow the spins to align along a common axis. In this way bulk magnetization measurements which determine the magnetic moment of the whole sample may be used to determine saturation magnetization. An approximation for the approach to saturation may be given by

$$M = M_s (1-b/H_o) + \chi H_o$$

(McGuire and Flanders 1969). The constant b is a measure of the energy required to rotate the domains with an external field H_o. χ is the diamagnetic susceptibility contribution from the core electrons in the sample. Contributions to the magnetization from sample holders, etc. would also be contained in this term. If b is small so that the magnetic material saturates easily, then for large magnetic fields the M versus H_o curve becomes linear. An extrapolation of the linear portion to H_o = 0 gives the saturation magnetization M_s. An example of this is shown in Figure 4.

CHAPTER 3

SAMPLE PREPARATION AND EXPERIMENTAL APPARATUS

This section is divided into two parts. The first part concerns sample preparation while the second part describes the apparatus used in making the measurements.

SAMPLE PREPARATION

Eleven samples of different compositions between Ni_2MnSn and Cu_2MnSn were prepared. These can be represented by the formula $Ni_xCu_{2-x}MnSn$ with $x = 2, 1.8, 1.6, ---- 0.2, 0$. The starting Ni, Cu, Mn, and Sn were weighed out to within 0.5 milligrams of the amount required. Since thirty gram samples were made this corresponds to a maximum contribution of 0.01% to the composition error. The constituents were melted in an R.F. induction furnace in Al_2O_3 crucibles. The atmosphere was a slight overpressure of argon to prevent oxidation and vaporization. After several minutes of homogenization in the melt the alloys were cooled slowly to room temperature. The resulting ingots were then broken into convenient size pieces, some of which were ground into 325 mesh powder. Then, several small chunks of alloy and the powder were sealed in quartz tubes under vacuum after flushing twice with helium. These sealed tubes were used for annealing the samples.

To prevent oxidation it is best not to anneal fine powders, however, it is necessary so that samples used for X-rays and samples

used for magnetization measurements have undergone identical heat treatments. Also, annealing the powder removes cold work strains induced by grinding. The sealed tubes were evacuated well enough so that no problems with oxidation were experienced.

The alloys were annealed in two sets. The group Ni_2MnSn to NiCuMnSn were annealed for ten days at 700° C while the rest were annealed for ten days at 550° C. The copper-rich alloys were annealed at a lower temperature because their melting point is lower than that for the nickel-rich alloys. Cu_2MnSn was observed molten at 700° C. All samples were quenched into water from the annealing temperature. It was noted that Cu_2MnSn was nonferromagnetic before annealing and strongly ferromagnetic after. All other samples were ferromagnetic both before and after annealing. For the X-ray diffractometer part of the annealed powders were pressed onto flat plate glass microscope slides using Dow Corning vacuum grease as a binder. Samples for the magnetometer were prepared from selected annealed pieces of alloy. The pieces used were less than one-quarter inch long in any one dimension and were mounted on the end of four millimeter quartz rods with ceramic cement[*]. A similar rod with cement but without a sample was used for standardization purposes.

---

[*]Sauereisen Cements Company, Pittsburg, Penna.

DESCRIPTION OF APPARATUS

X-RAY DIFFRACTOMETER

Lattice parameters were measured using a vertical powder X-ray diffractometer. The goniometer head was rotated slowly by a stepping motor at a constant rate of one degree per eight minutes while signals from the detector were processed by a Phillips ratemeter. Copper K-alpha radiation was used with a Ni filter. Information from the ratemeter was recorded by a chartrecorder resulting in a diffraction pattern of two centimeters per degree dispersion. The scale of the chartrecorder and the position of the goniometer tracked accurately over a one-hundred degree span and this was checked for each sample. The absolute accuracy of the lattice parameters measured by this method was not determined, however, the results were consistent if any sample was measured twice. The lattice parameters obtained for the end members Ni_2MnSn and Cu_2MnSn agree with the published values. This is shown in Chapter 4 in the section on X-ray diffractometer data.

ELECTRON MICROPROBE

Composition of the samples was checked using standard electron microprobe analysis.

VIBRATING SAMPLE MAGNETOMETER

Magnetic measurements were done using a Princeton Applied Research vibrating sample magnetometer. The required magnetic fields were obtained using a Magnion water cooled electromagnet which could be ramped at a constant rate to approximately fifteen kOe. Low temperature measurements were done using an Andonian Assoc. liquid helium dewar while high temperature measurements were done using a vacuum walled furnace. In both cases heaters were controlled by a proportional temperature controller monitoring a chromel versus gold-0.07 atomic percent iron thermocouple at low temperatures and a copper constantan thermocouple for temperatures up to four-hundred degrees centigrade. For higher temperatures a platinum versus platinum-10 atomic percent rhodium thermocouple was used. Voltages proportional to magnetization and applied field or magnetization and temperature were measured by two digital voltmeters whose digital outputs were monitored by a Texas Instruments 960A on-line mini-computer. The resulting computer output was a histogram of magne-tization versus field or magnetization versus temperature. The magnetometer was calibrated using a pure Ni sample of mass 0.07507 grams as a standard. Using the accepted value of 55.11 ± 0.06 emu per gram at $4.2°$ K for the magnetic moment of pure nickel (Crangle and Goodman 1971) a calibration constant for the magnetometer was calculated. This varied between 1.46 and 1.47 emu per volt and was checked periodically.

ANDONIAN DEWAR

This dewar used for low temperature measurements is of a design which allows the temperature to be varied continuously from $4.2°$ K to room temperature. This is accomplished by bubbling liquid helium through the sample chamber which is surrounded by a heater. This way the sample is not in contact with the liquid helium bath but is cooled by helium gas to the required temperature.

CHAPTER 4

DATA

X-RAY MEASUREMENTS

X-ray measurements for all samples were done using a slow scan
speed of eight minutes per degree. All samples were found to have the
$L2_1$ structure showing the expected F.C.C. lines in the diffraction
pattern. Lattice parameters were found by averaging those calculated
from the higher order lines in each diffraction pattern. Some samples
were checked by step scanning one or more of the higher order peaks.
A typical step scanned peak is shown in Figure 2.

The lattice parameters are thought to be accurate to at least
0.01 Å. The value of 6.053 Å obtained for Ni_2MnSn is in good agree-
ment with the 6.052 Å measured by Webster (1968) while the extra-
polated value of 6.164 Å for Cu_2MnSn compares favorably with the 6.161
Å measured by Carapella and Hultgren (1942). More importantly the
measure of variation in lattice parameter from sample to sample is
thought to be accurate to better than 0.005 Å. This is because sys-
tematic errors resulting from diffractometer alignment are the same
for all samples. Several samples were analysed twice on separate dif-
fractometer runs and in all cases the measurements were within 0.005
Å. A summary of all lattice parameter measurements is shown in Table
1 and a plot of the variation with composition is shown in Figure 3.

Figure 2

The (422) X-ray powder diffraction peaks for $Ni_{1.6}Cu_{0.4}MnSn$ as measured by step scanning. These peaks are typical of those seen for the alloys when measuring lattice parameters.

Table 1

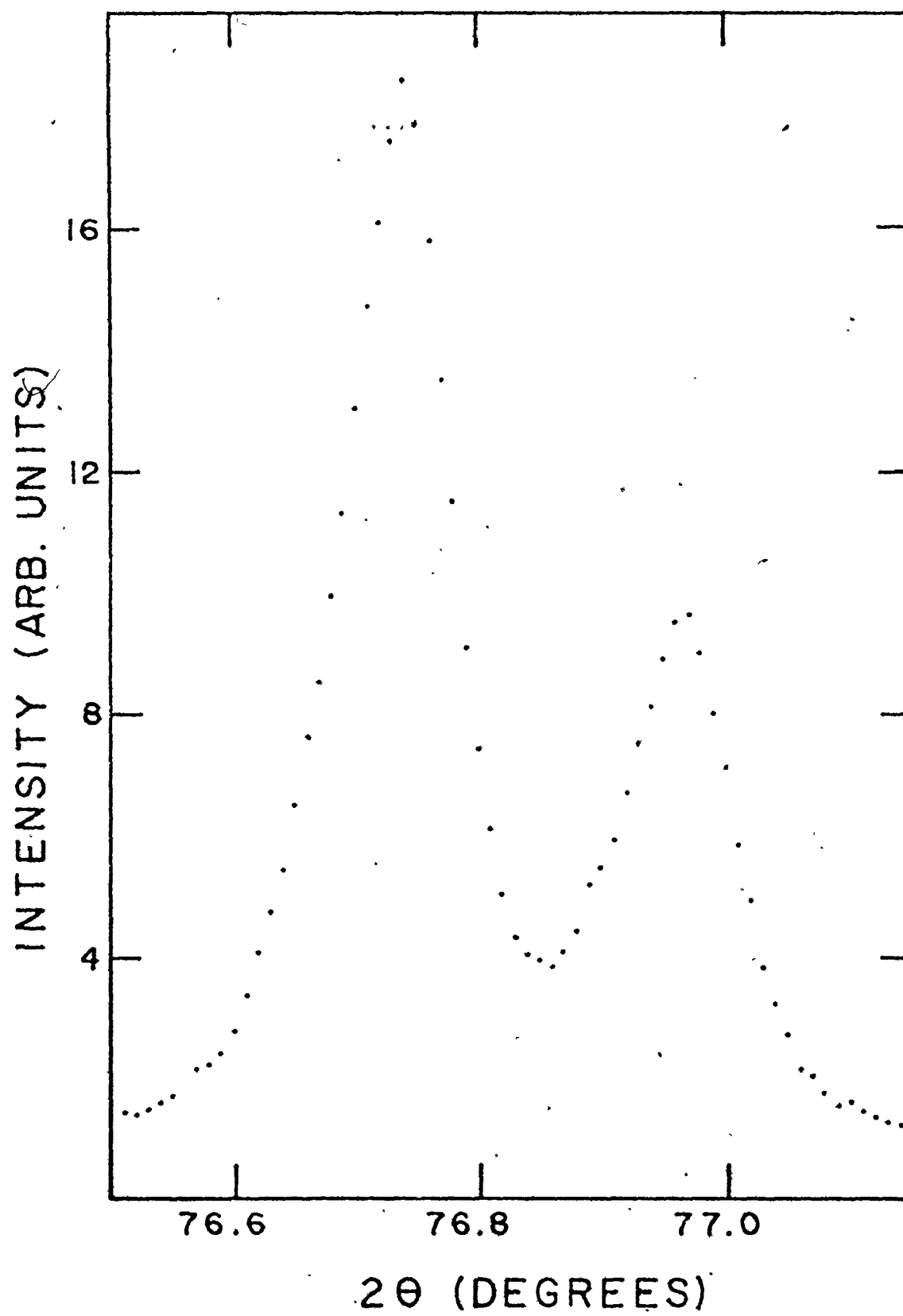The lattice parameters of $Ni_xCu_{2-x}MnSn$ measured
in angstroms. The value obtained for Cu_2MnSn
is from the extrapolation of Figure 3. The
experimental error for all lattice parameters is
estimated to be ±0.005 Å.

TABLE 1

Lattice parameters of

$Ni_xCu_{2-x}MnSn$

x	LATTICE PARAMETER (angstroms)
2.0	6.053 ± 0.005
1.8	6.063
1.6	6.076
1.4	6.087
1.2	6.100
1.0	6.105
0.8	6.118
0.6	6.132
0.4	6.145
0.2	6.153
0.0	6.164

Figure 3

A plot of the composition dependence of the

lattice parameters for $Ni_xCu_{2-x}MnSn$.
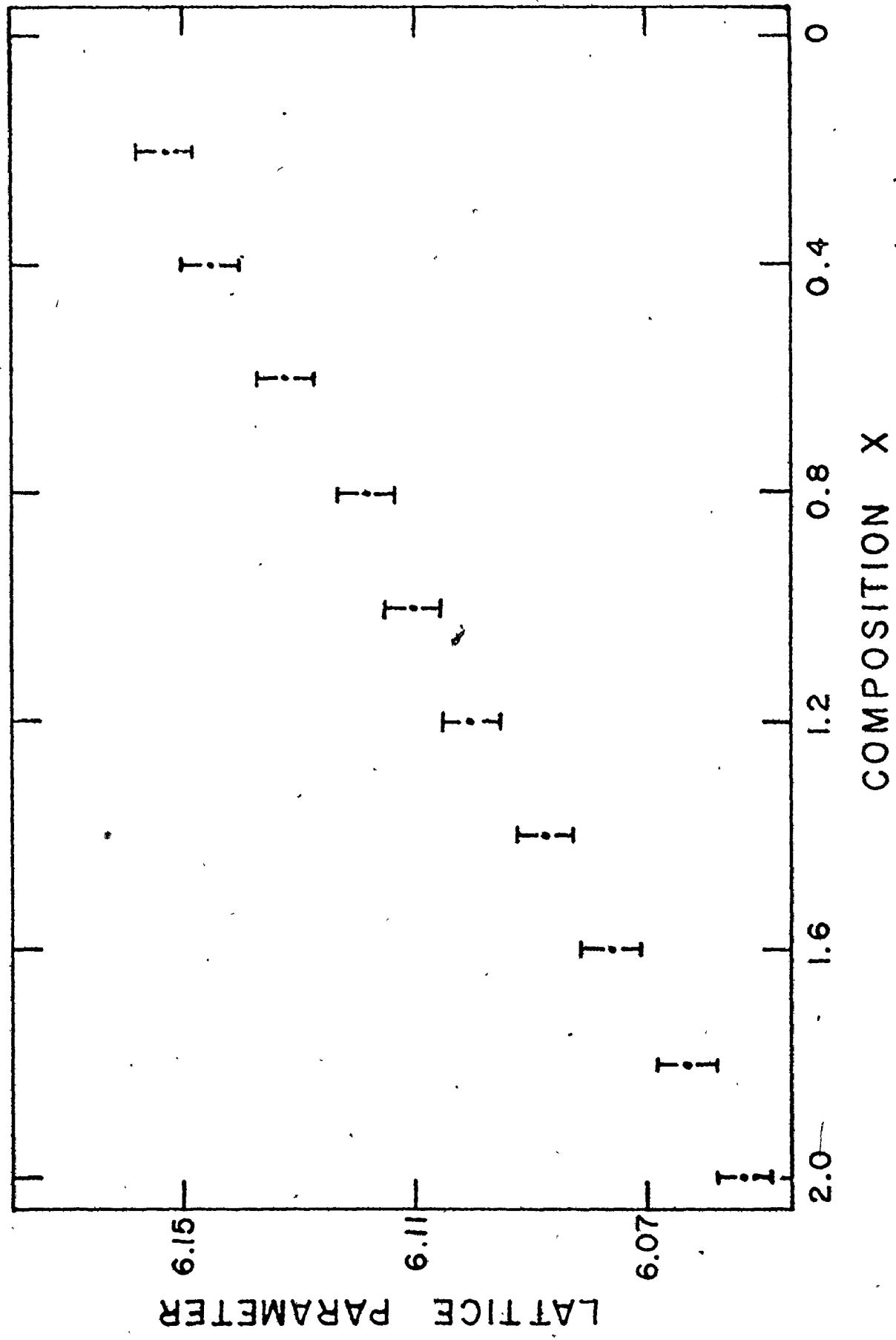
MICROPROBE ANALYSIS

A check on the composition of some of the samples was done using an electron microprobe. This apparatus bombards the sample with a one square micron beam of high energy electrons. The spectrum of the emitted X-rays was obtained and the elements of the sample found by identifying their characteristic wavelengths. A computer program calculates the composition from the relative intensities. The electron beam could be scanned across the sample allowing a check of homogeneity. All samples analysed were found to be within ten percent of their nominal composition and this is close to the limits of experimental error for this device. Variations in composition of no more than five percent were found when scanning across several samples.

MAGNETIZATION MEASUREMENTS

Field runs to determine saturation moments were done on all samples except Cu_2MnSn which was eliminated because of instability of the quenched high temperature $L2_1$ phase. Saturation moments were determined at temperatures from $4.2°$ K up to the Curie temperature for each sample. A plot of magnetization versus applied field is shown in Figure 4 for NiCuMnSn. A complete list of results for all field runs at all temperatures is given in Table 2.

For each alloy, saturation moment versus temperature was plotted to check that the magnetization of the samples fell off smoothly with increasing temperature up to T_c. This provided a check for unwanted phases and two component systems. Magnetization fell smoothly

Figure 4

Graph showing the variation of the magnetization of NiCuMnSn with the applied field H at 4.2° K. Note that the M = 0 point is not shown. This graph illustrates the method used to determine saturation moments for the alloys.

MAGNETIZATION (EMU/GRAM)
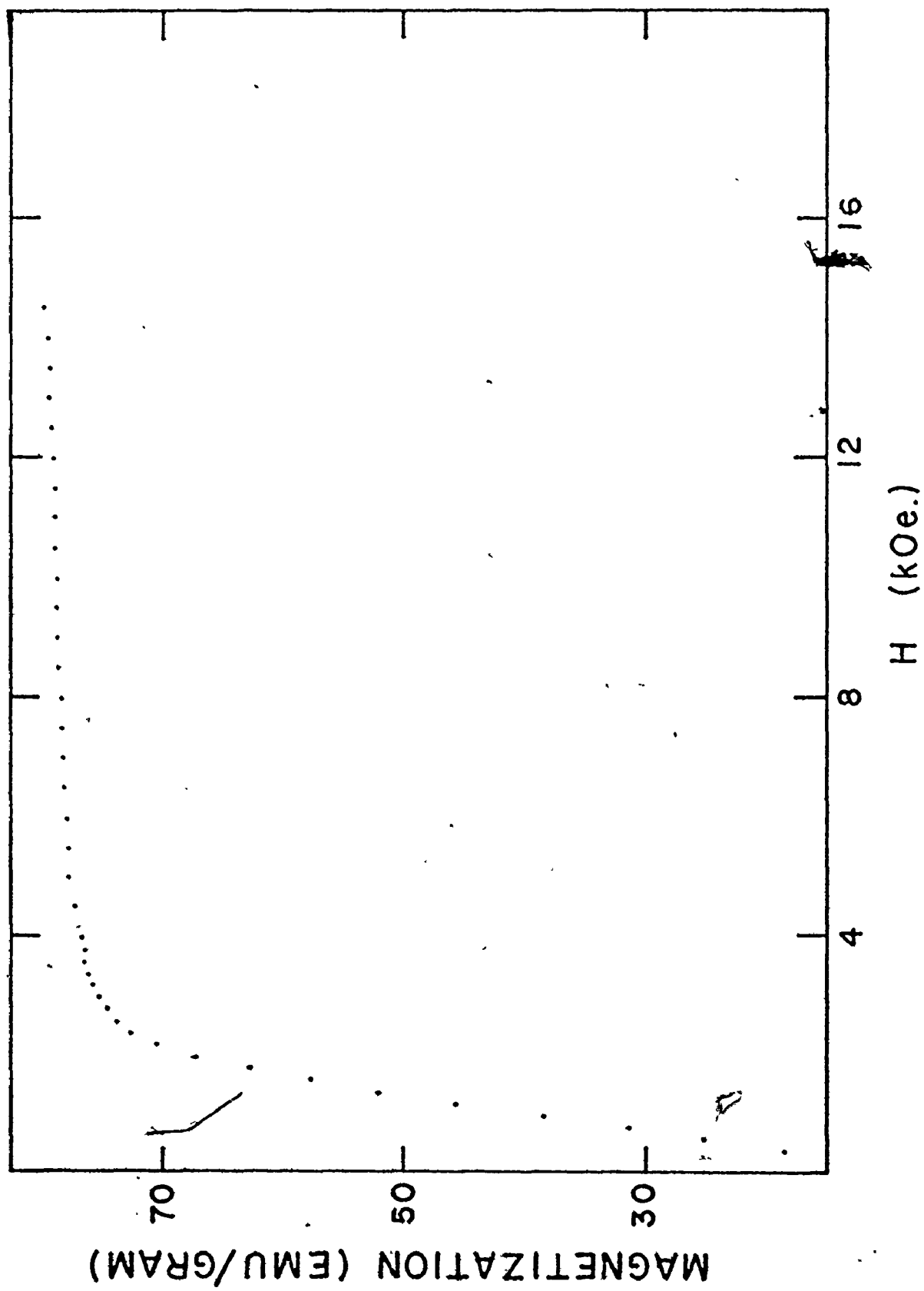
H (kOe.)

Table 2

Saturation magnetization measurements for

$Ni_xCu_{2-x}MnSn$.

TABLE 2

Saturation magnetization of $Ni_xCu_{2-x}MnSn$

x = 0.2		x = 0.4		x = 0.6	
T (° K)	M (u_B/Mn)	T (° K)	M (u_B/Mn)	T (° K)	M (u_B/Mn)
4.2	3.72	4.2	3.90	4.2	4.04
75	3.67	76	3.83	74	3.97
149	3.57	149	3.73	149	3.78
224	3.45	224	3.53	224	3.51
296	3.18	298	3.27	296	3.17
372	2.87	373	2.82	324	2.97
423	2.58	423	2.35	348	2.78
474	2.11	454	1.92	372	2.51
504	1.65			398	2.15
523	1.15			422	1.62

x = 0.8		x = 1.0		x = 1.2	
T (° K)	M (u_B/Mn)	T (° K)	M (u_B/Mn)	T (° K)	M (u_B/Mn)
4.2	4.02	4.2	4.10	4.2	4.04
75	3.91	50	4.03	101	3.81
174	3.60	101	3.91	200	3.33
224	3.36	151	3.70	281	2.54
296	2.86	2000	3.47	296	2.30
322	2.59	249	3.13	313	2.06
348	2.30	296	2.61	333	1.60

TABLE 2 -- Continued

372	1.81	313	2.38
398	1.01	333	2.01

x = 1.4		x = 1.6		x = 1.8	
T (° K)	M (u_B/Mn)	T (° K)	M (u_B/Mn)	T (° K)	M (u_B/Mn)
4.2	4.04	4.2	4.07	4.2	4.04
100	3.83	100	3.86	100	3.88
200	3.33	200	3.36	200	3.41
297	2.27	296	2.30	294	2.38
318	1.85	312	2.16	315	1.90
331	1.38	333	1.19	333	1.16

x = 2.0	
T (° K)	M (u_B/Mn)
4.2	4.07
100	3.90
200	3.44
296	2.40
313	2.07
328	1.59

for all samples. A plot is shown for several of the samples in
Figure 5.

To measure the Curie point of the samples, they were heated
past T_c and allowed to cool through the Curie point in a field of
approximately 500 Oe. A plot of the resulting signal is shown in
Figure 6 for two different samples. The method of extrapolation to
determine T_c is evident from the figure. This method was checked by
doing an Arrott plot for a similar sample. Agreement was within one
degree K. A list of all data is given in Table 3. Figure 7 shows a
plot of Curie temperature T_c versus composition x for $Ni_xCu_{2-x}MnSn$.

After the Curie points were determined the samples were heated
in a constant field of 10.9 kOe to determine the paramagnetic moments
and the paramagnetic Curie temperatures. The samples were heated up
to the temperature at which they were annealed. This poses a problem
for the Cu-rich samples because for these samples the melting point
approaches Tc. This results in a relatively small linear portion of
the curve when inverse magnetization is plotted versus temperature.
Since P is determined from the slope of the linear part, values for P
are less reliable as the samples become more Cu-rich. A plot to deter-
mine θ and P for one of the samples is shown in Figure 8 while a list
of all high temperature data is given in Table 3. Figure 9 shows a
plot of P versus composition x and Figure 10 shows the dependence of
θ on composition x.

Figure 5

Saturation magnetization versus temperature for:

$$1 - Ni_{0.2}Cu_{1.8}MnSn$$

$$2 - Ni_{0.6}Cu_{1.4}MnSn$$
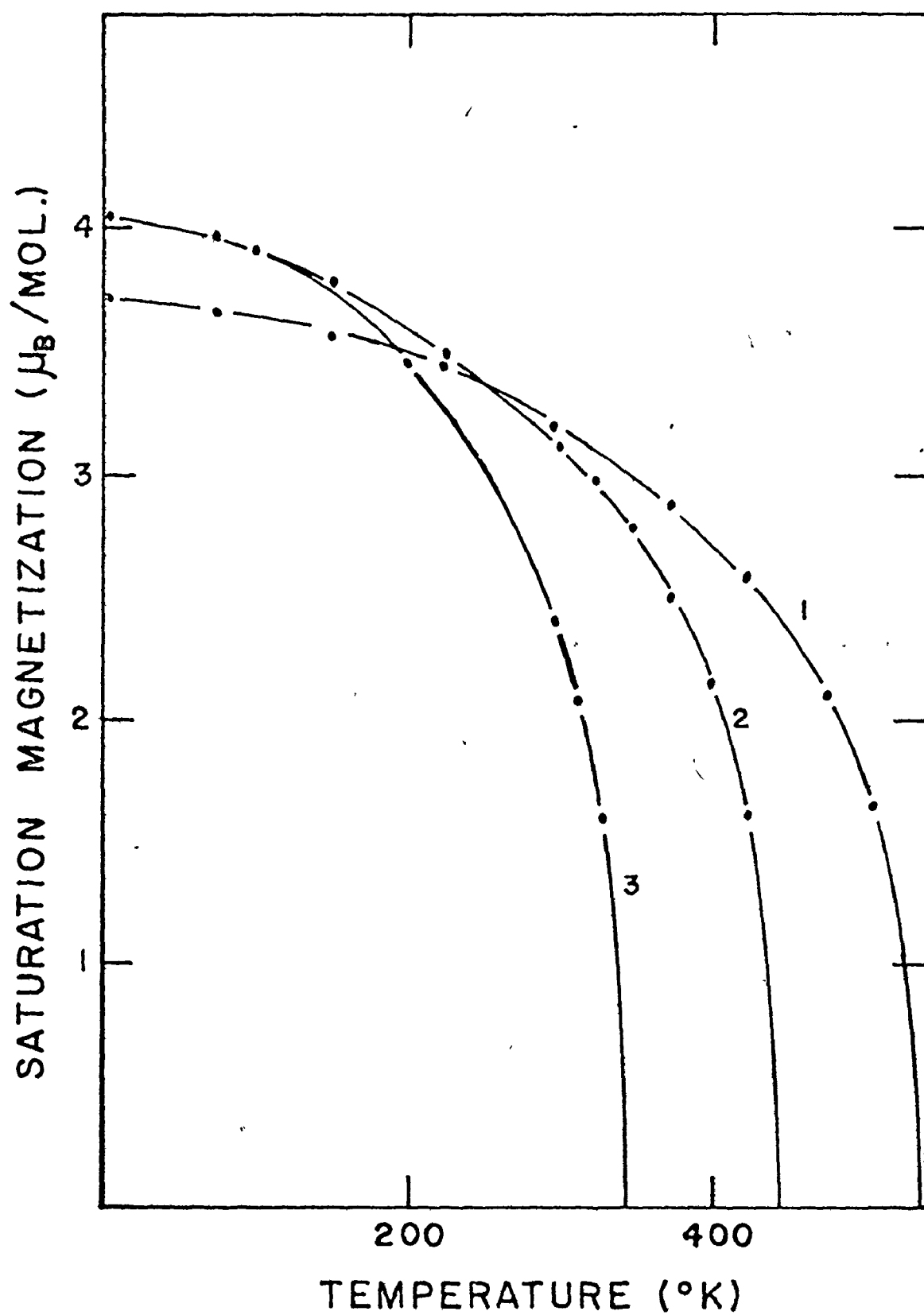
$$3 - Ni_2MnSn$$

The curves are extrapolated to $M = 0$ at $T = T_c$.

Figure 6

Remnant magnetization versus temperature for:

1 - NiCuMnSn

2 - $Ni_{0.6}Cu_{1.4}MnSn$

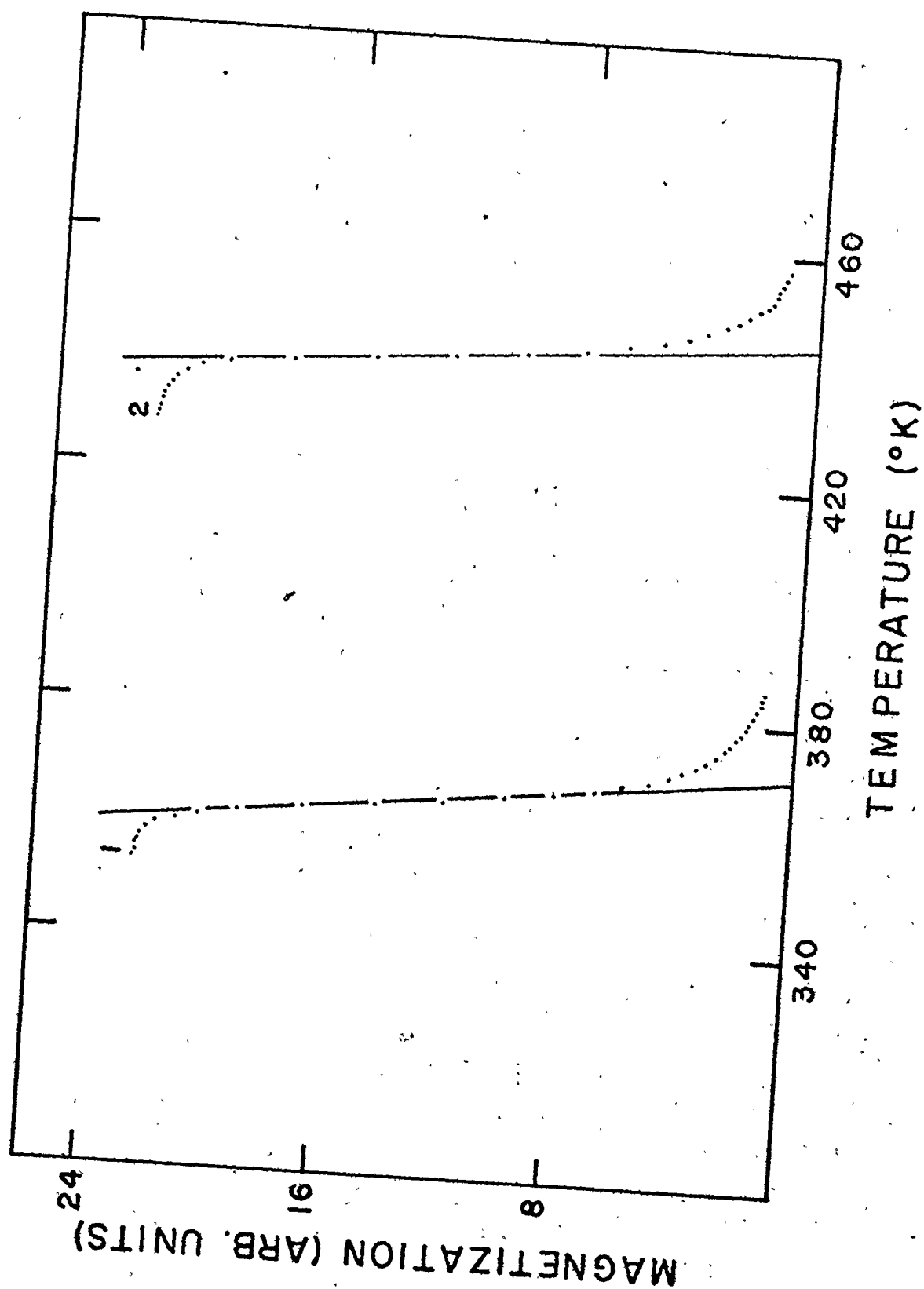The solid line illustrates the method of extrapolation

for obtaining T_c.

Table 3

P, θ_c, and T_c for the Heusler alloys $Ni_xCu_{2-x}MnSn$.

TABLE 3

High temperature results for $Ni_xCu_{2-x}MnSn$

x	P $(u_B$/molecule)	θ_c (° K)	T_c (° K)
2.0	5.00 ± .10	365 ± 10	346 ± 2
1.8	4.92	373	342
1.6	4.84	388	341
1.4	4.67	423	345
1.2	4.60	448	350
1.0	4.35	473	370
0.8	4.19	503	403
0.6	4.08	533	445
0.4	3.74	568	492
0.2	3.30	583	538
0.0	--	--	--

Figure 7

Graph showing the variation of Curie temperature

T_c with composition x for $Ni_xCu_{2-x}MnSn$.

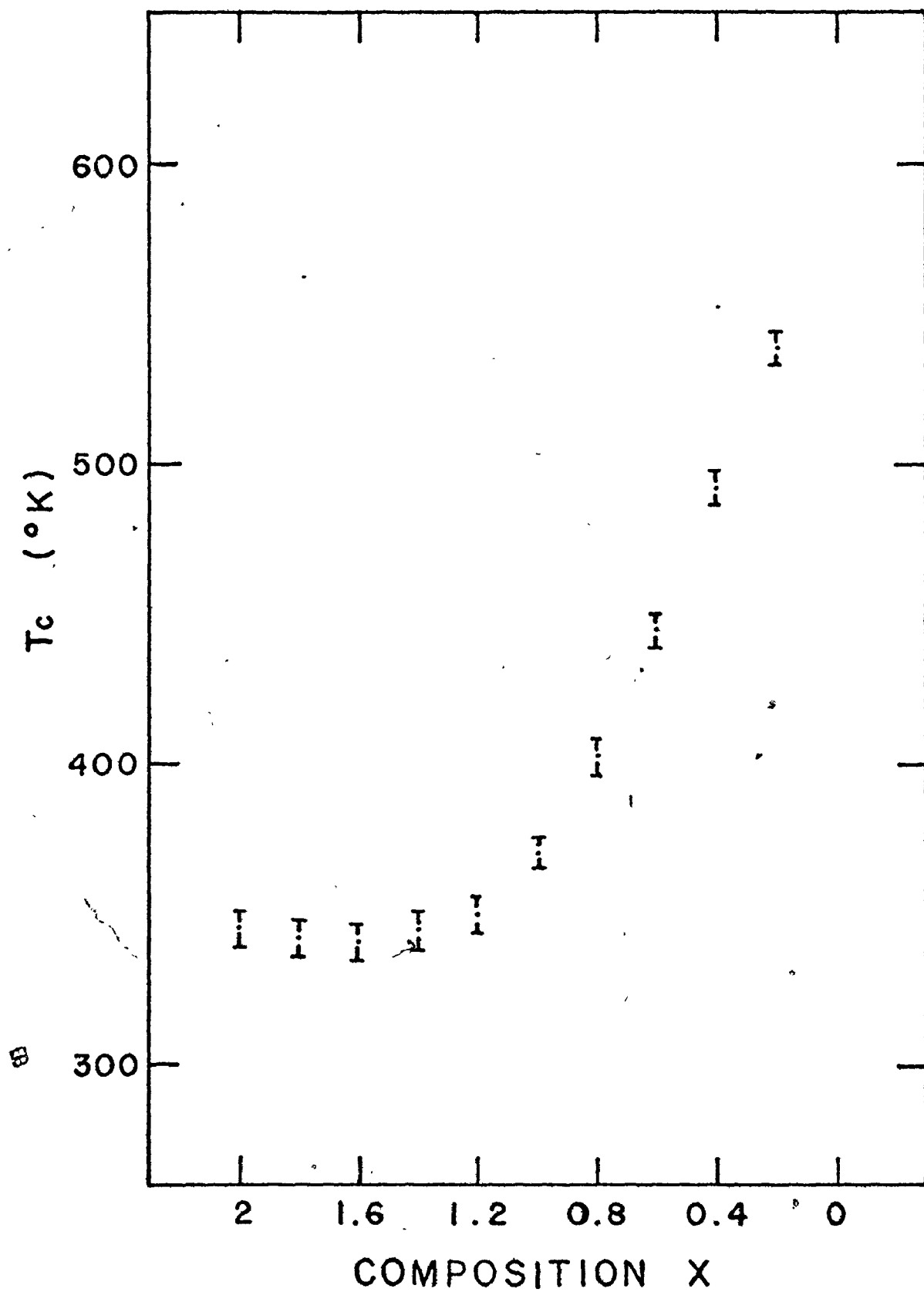Figure 8

A plot of inverse magnetization versus

temperature for $Ni_{1.4}Cu_{0.6}$InSn in an applied

field of 10.9 kOe.   The solid line illustrates
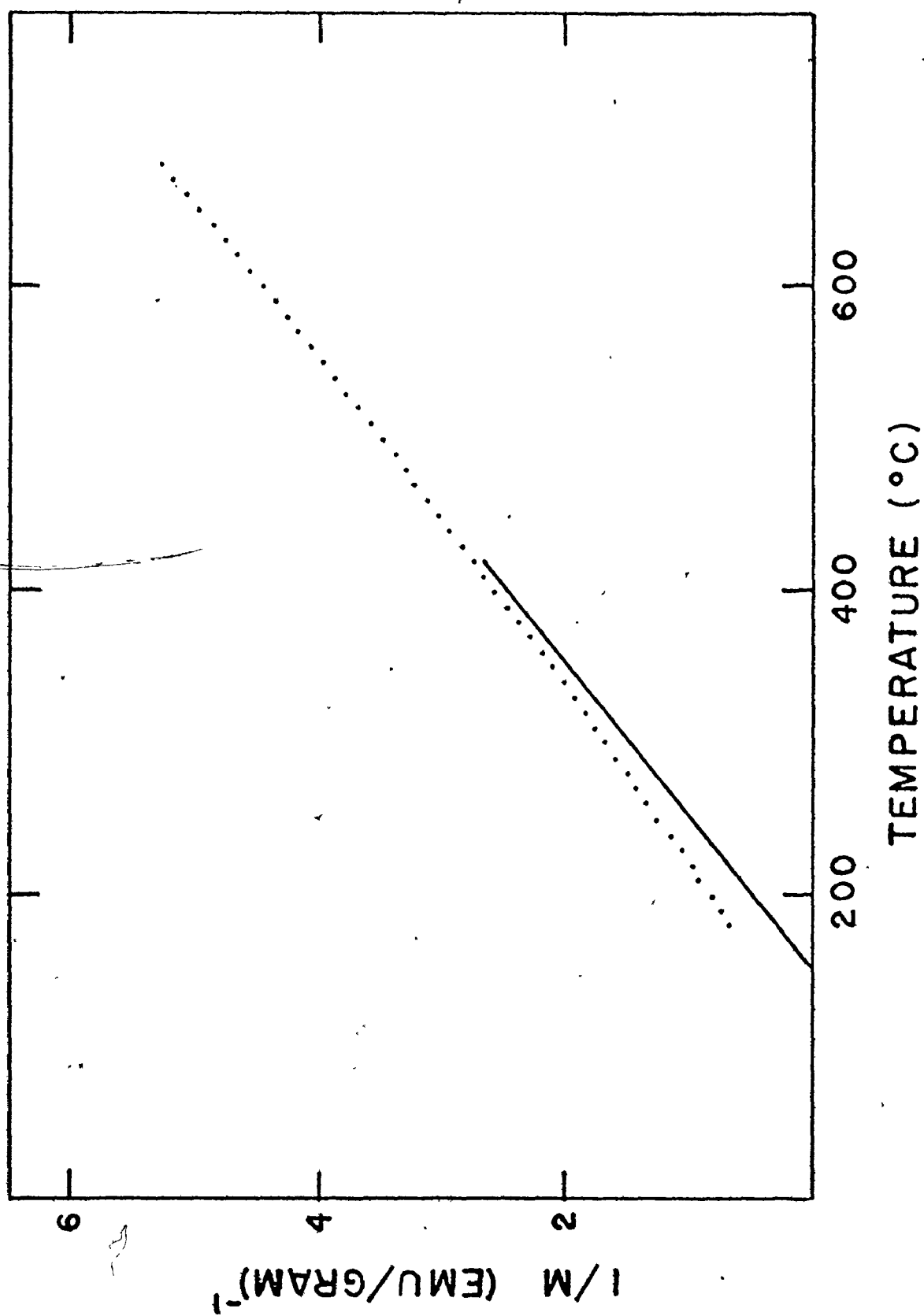
the method of extrapolation for determining θ.

Figure 9

Graph showing the variation of the paramagnetic

moment P with the composition x for $Ni_xCu_{2-x}MnSn$.

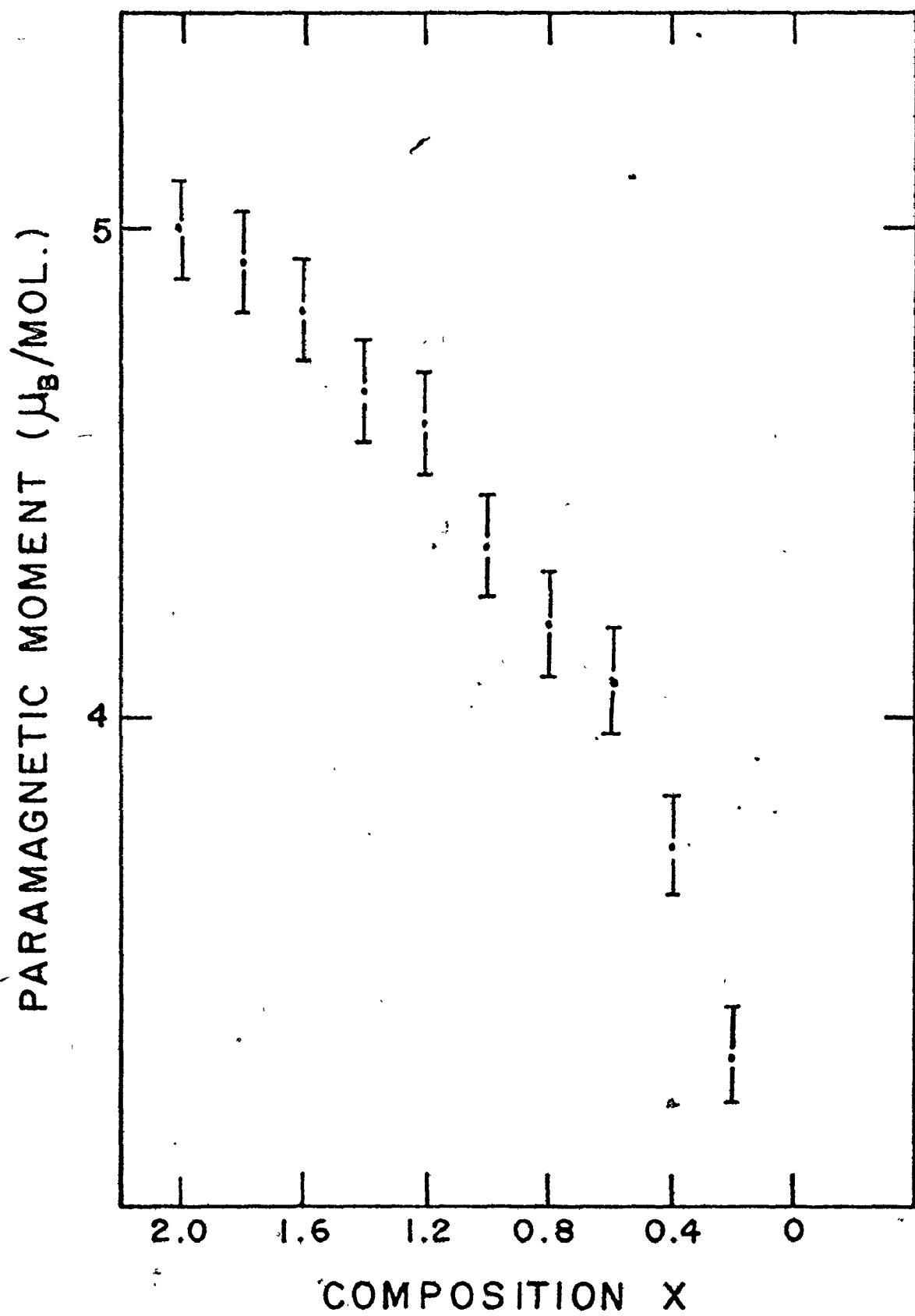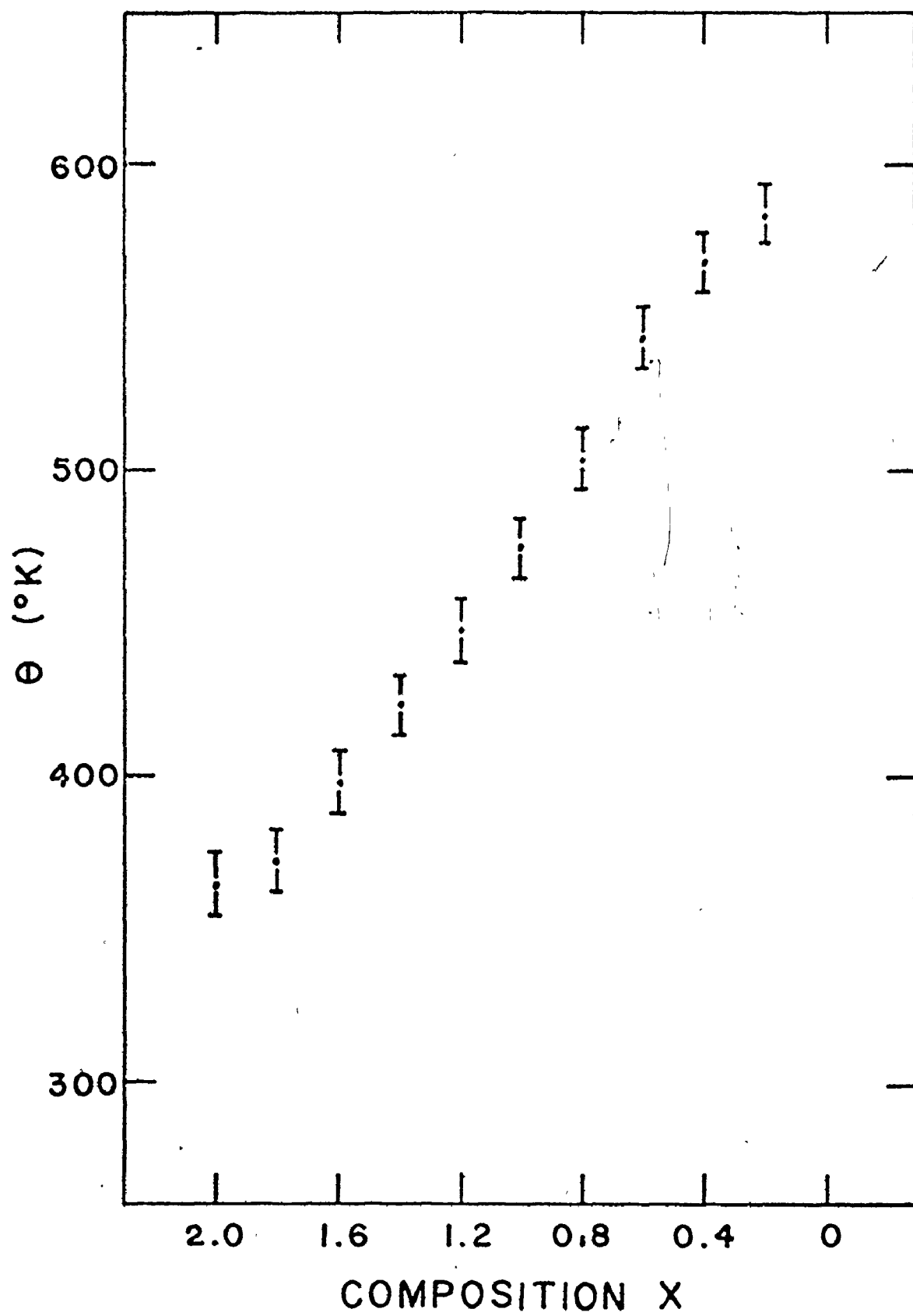Figure 10

A plot of the variation of the paramagnetic

Curie temperature θ with composition x for

$Ni_x Cu_{2-x} MnSn$.

CHAPTER 5

DISCUSSION

The X-ray measurements show that the system of alloys $Ni_xCu_{2-x}MnSn$ remain stable in the Heusler $L2_1$ phase even for high copper concentrations. Although the alloy Cu_2MnSn is unstable and precipitates other phases when heated, $Ni_{0.2}Cu_{1.8}MnSn$ and the other alloys appear not to show this effect. This is supported by the observation that all the samples containing nickel were ferromagnetic both before and after annealing. Also an X-ray diffraction pattern of an unannealed powder of $Ni_{0.2}Cu_{1.8}MnSn$ showed only slight traces of impurity phases. These did not disappear when the powder was annealed and quenched so they are probably not due to precipitation. All nine other alloys from $x = 0.4$ to $x = 2.0$ are entirely Heusler and show well defined Curie temperatures in remnant magnetization versus temperature plots. The lattice parameters are seen to vary linearly from 6.053 Å for Ni_2MnSn to 6.164 Å for Cu_2MnSn. This linear variation is evidence that the composition varies smoothly from sample to sample. The absence of any additional diffraction peaks or any broadening supports the view that the alloys are homogeneous. The saturation magnetization remains constant at 4.0 ± 0.1 u_B/molecule throughout the composition range except for $Ni_{0.2}Cu_{1.8}MnSn$ at 3.71 u_B/molecule. This slight drop in saturation moment is probably due to the presence of the small amount of impurity phases seen by X-ray diffraction.

31

Some difficulties were encountered when measuring the para-
magnetic moments P and the paramagnetic Curie temperatures θ. One
problem is that as the copper concentration is increased T_c increases
rapidly until at $Ni_{0.2}Cu_{1.8}MnSn$ T_c is only a few hundred degrees
lower than the melting point. Molecular field theory requires high
temperatures for a determination of P and θ but measurements become
difficult in this region because of the small signals produced by the
samples when they are paramagnetic. A rule of thumb for measurements
in the paramagnetic region is to use temperatures greater than 2 T_c
but this is impossible for the copper-rich alloys because of their
high Curie temperatures. Figure 8 illustrates the method used to
obtain the data.

The paramagnetic moment appears to drop rapidly as the copper
end of the composition range is approached. This effect is real and
not a result of the difficulties mentioned above. If it were possible
to extend the temperature range of the measurements, P would decrease
since the slope of the 1/M versus T graph increases monotonically over.
the accessible temperature range. This means that the measurements
determine an upper estimate to the actual value of the paramagnetic
moments.

It is unusual that P drops so suddenly when the saturation
moment stays constant. This could result if the alloys underwent some
form of disorder as they were heated. This disorder would have to be
completely reversible since several of the alloys were measured again
at low temperatures and gave exactly the same saturation moments as
before. Ni_2MnSn is known to disorder when annealed above 1000° C and

quenched to room temperature. Campbell and Stager (1976) state that the Mn-Sn disorder leads to manganese near neighbour pairs that are close enough for a direct antiferromagnetic interaction. Although no detailed calculations have been carried out it is expected that this will cause the observed curvature in the $1/M$ versus T plot.

The Curie temperature T_c varies nonlinearly with composition as shown in Figure 7. This seems to suggest that something unusual is happening to the electronic structure of the crystal as the composition is changed. It is expected that the conduction band electron concentration varies linearly as the copper concentration is increased and, if this is the case, some other mechanism may be responsible for the interactions which determine T_c.

The paramagnetic Curie temperature θ appears to vary linearly with composition, however the measurements of θ are estimated to be low because of the curvature of the $1/M$ versus T curves at high temperature. This curvature is presumably caused by disorder.

CHAPTER 6

CONCLUSIONS

The magnetic properties of the system of Heusler alloys $Ni_xCu_{2-x}MnSn$ have been measured from $4.2°$ K to more than $900°$ K. The Heusler phase of the alloys has been found stable at high copper concentrations even though Cu_2MnSn is unstable. The effective paramagnetic moment appears to drop as the copper concentration is increased and this is attributed to disorder at high temperatures. The variation of T_c with composition of the X site component is seen to be nonlinear suggesting unusual changes in the electronic properties of the alloys. Calculations of the band structure seem necessary for the interpretation of the results, however it is apparent that the X site plays an important role in determining the interactions responsible for the difference in Curie temperatures among the Heusler alloys.

BIBLIOGRAPHY

1. Booth, J.G. and Pritchard, R.G., 1975 J. Phys. F. 5, 347.

2. Campbell, C.C.M., 1975 J. Phys. F. 5, 1931.

3. Campbell, C.C.M. and Stager, C.V., 1976 Submitted to Can. J. Phys.

4. Carapella, L.A. and Hultgren, R., 1942 Trans. AIME 147, 232.

5. Caroli, B. and Blandin, A., 1966 J. Phys. Chem. Solids 27, 503.

6. Crangle, J. and Goodman, G.M., 1971 Proc. Roy. Soc. Lond. A. 321, 477.

7. Endo, K. et al., 1972 J. Phys. Soc. Japan 32, 285.

8. McGuire, T.R. and Flanders, P.J., Magnetism and Metallurgy Volume One, p. 128. Academic Press, New York and London, 1969.

9. Noda, Y. and Ishikawa, Y., 1976 J. Phys. Soc. Japan 40, 690.

10. Oxley, D.P. et al., 1963 J. Appl. Phys. 34, 1362.

11. Smart, J.S., Effective Field Theories of Magnetism, W.B. Saunders Company, Philadelphia and London, 1966.

12. Webster, P.J. and Tebble, R.S., 1967 Phil. Mag. 16, 347.

13. Webster, P.J. and Tebble, R.S., 1968 J. Appl. Phys. 39, 471.

14. Ziebeck, K. and Webster, P.J., 1974 J. Phys. Chem. Solids 35, 1.